

2003

## Coupled seismic slip on adjacent oceanic transform faults

Donald W. Forsyth

Yingjie Yang

Maria-Daphne Mangriotis

Yang Shen

*University of Rhode Island*, [yshen@uri.edu](mailto:yshen@uri.edu)

Follow this and additional works at: <https://digitalcommons.uri.edu/gsofacpubs>

Terms of Use

All rights reserved under copyright.

---

### Citation/Publisher Attribution

Forsyth, D. W., Y. Yang, M.-D. Mangriotis, and Y. Shen (2003), Coupled seismic slip on adjacent oceanic transform faults, *Geophys. Res. Lett.*, 30, 1618, doi: 10.1029/2002GL016454, 12.

Available at: <https://doi.org/10.1029/2002GL016454>

This Article is brought to you for free and open access by the Graduate School of Oceanography at DigitalCommons@URI. It has been accepted for inclusion in Graduate School of Oceanography Faculty Publications by an authorized administrator of DigitalCommons@URI. For more information, please contact [digitalcommons-group@uri.edu](mailto:digitalcommons-group@uri.edu).

---

## Coupled seismic slip on adjacent oceanic transform faults

Terms of Use

All rights reserved under copyright.

## Coupled seismic slip on adjacent oceanic transform faults

Donald W. Forsyth, Yingjie Yang, and Maria-Daphne Mangriotis

Dept. of Geological Sciences, Brown Univ., Providence, Rhode Island, USA

Yang Shen

Graduate School of Oceanography, Univ. of Rhode Island, Narragansett, Rhode Island, USA

Received 15 October 2002; revised 19 December 2002; accepted 30 January 2003; published 20 June 2003.

[1] In a four and a half hour period, more than 60 events in an earthquake swarm on the western boundary of the Easter microplate were detected by an array of ocean bottom seismometers. The larger events of the swarm were strike-slip earthquakes located on two transform faults separated by about 25 km. Slip on the faults was closely coupled, with activity alternating back and forth randomly between the two transforms. Coupled seismic activity is usually attributed to triggering by static stress changes or dynamic stresses in propagating shear waves generated by another earthquake, but these earthquakes are too small for either mechanism to be plausible. We suggest that the swarm may have been the seismic manifestation of a larger, primarily aseismic, slip event or slow earthquake involving both transforms, perhaps triggered by dike injection on the Easter-Pacific spreading center. **INDEX TERMS:** 3035 Marine Geology and Geophysics: Midocean ridge processes; 7209 Seismology: Earthquake dynamics and mechanics; 7223 Seismology: Seismic hazard assessment and prediction; 7230 Seismology: Seismicity and seismotectonics. **Citation:** Forsyth, D. W., Y. Yang, M.-D. Mangriotis, and Y. Shen, Coupled seismic slip on adjacent oceanic transform faults, *Geophys. Res. Lett.*, 30(12), 1618, doi:10.1029/2002GL016454, 2003.

### 1. Introduction

[2] Large strike-slip earthquakes sometimes trigger seismicity on other faults or on other segments of the same fault [Hill *et al.*, 1993; Stein *et al.*, 1997; Gombert *et al.*, 2001]. Two mechanisms for this triggering have been suggested: changes in static stress accompanying slip; and transient, dynamic stresses in shear waves propagating away from the earthquake. In this paper, we demonstrate that in a single earthquake swarm, closely coupled, strike-slip displacement occurred on two parallel transform faults, separated by about 25 km on the spreading center boundary between the Pacific plate and the Easter microplate. The earthquakes in this swarm are too small for either static stress changes or transient shear waves to be plausibly responsible for the coupling. The nearly simultaneous slip on two faults may support the hypothesis that large, slow earthquakes on oceanic transforms sometimes slip on more than one fault strand [McGuire *et al.*, 1996; McGuire and Jordan, 2000], a suggestion that has been challenged recently [Abercrombie and Ekstrom, 2001].

[3] Three events in the swarm of December 3, 1995 on the southern East Pacific Rise were catalogued in the

routine earthquake bulletins with  $m_b$  3.9, 4.7 and 4.1, respectively [Bull. Int. Seism. Center, 1995]. In addition, nearby events of magnitude about 4.0 were reported approximately 2 months and 9 months after the swarm. There were, however, many other events large enough for the surface waves to be detected, even though the P and S waves normally used in locating events did not stand out above the noise level. In a four-and-a-half-hour period including all three of the reported events, surface waves from 24 events can be detected on records from the nearest island station, RPN (Figure 1), including several of about the same size as the first reported event.

[4] A temporary array of ocean-bottom seismometers (OBS), deployed as part of the MELT Experiment [MELT Seismic Team, 1998], greatly enhanced our ability to detect and locate events within the swarm. All OBSs in the array (Figure 1) were equipped with either differential pressure gauges (DPG) or hydrophones and many also had three-component seismometers. Our analysis focuses on T-phases or hydroacoustic waves travelling in the water column recorded at nearby station RPN and the OBS array; and Rayleigh and Love surface waves recorded at quieter stations of the Global Seismic Network as well as on the DPGs or seismometers of the array. Using T-phases, we detected more than 60 events in the swarm.

### 2. Location Technique

[5] We determine the relative locations of events within the swarm using relative arrival times of T-phases, Rayleigh waves and Love waves. Both T-phases and surface waves propagate horizontally with low phase velocity, yielding excellent constraints on epicentral location, but poor depth control. The frequency-dependence of surface wave excitation could potentially constrain the depths, but only a very limited period range is above the noise level at most teleseismic stations for all but the largest event. The earthquakes excited strong, short-period (3–8 s) Love waves that travel at crustal velocities and were observed at the OBS array and RPN, indicating that the sources are within or near the base of the crust. In addition, in this fast spreading environment, the lithosphere is probably very thin and hot, so brittle fracture is not likely to extend into the mantle. We assume all events are at about the same depth, and solve only for origin time and the epicenter using relative event techniques. For the surface waves, we simply cross-correlate the waveforms of the reference event, chosen to be the largest event, with the waveforms of other events to find relative arrival times. In the frequency band we employ

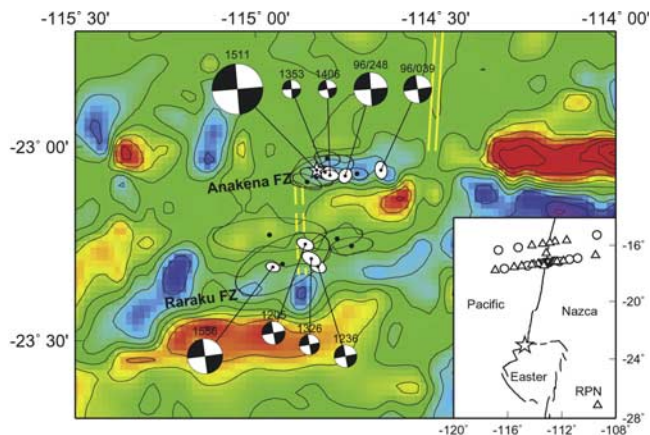


**Figure 1.** Locations and focal mechanisms of earthquakes in the swarm. Ellipses represent 95% confidence limits of locations relative to reference event (star). Filled ellipses are largest events for which mechanisms have been determined. Area of mechanism diagram is proportional to seismic moment, shaded quadrants represent compressional arrivals, and labels above diagrams indicate origin time or year and Julian day for events not part of the swarm. Colors indicate depth to seafloor, with red shades shallow and contour lines at 200 m intervals. Double yellow lines indicate location of spreading centers, dashed where uncertain. Inset shows location of seismometers (triangles) and differential pressure gauges (circles) of the MELT Experiment, Global Seismic Network station RPN, location of swarm (star) and plate boundaries.

(0.02–0.05 Hz) over a limited distance range in a mid-ocean ridge setting, dispersion is negligible compared to effects of changing location and is neglected. We use relative arrival times of surface waves only from station/event pairs with correlation coefficients  $>0.9$ ; the coefficient often exceeds 0.98.

[6] Waveforms of T-phases are too variable to cross-correlate successfully. Instead, we fit a simple functional form that describes the growth and gradual decay of T-phase energy to the log of the envelope of the T-phase. The peak of the function is considered to be the arrival time. This approach yields travel-time residuals and locations that are similar to those achieved by cross-correlating the energy envelopes directly [Shen, 2002]. 95% confidence regions for relative locations based separately on surface waves and T-phases overlap or nearly overlap, although we combine the two types of observations for the epicenters reported here. Velocities of the medium are taken from the best regression of arrival time versus distance for T-phases and from the characteristic phase velocities for surface waves in young seafloor of the East Pacific Rise [Nishimura and Forsyth, 1989]. In the combined locations, each observation is assigned an error equal to the standard deviation of either the T-phase or surface wave residuals. For the larger earthquakes, data importances indicate that the T-phase data contribute about 36% of the location information, but this fraction increases for smaller events as the surface waves are increasingly swamped by noise.

[7] The bulletin location of the largest earthquake of the sequence lies about 10 km south of the topographic trough

of the Anakena transform. Although this absolute location is known with much less accuracy than the precision of the relative locations, T-phase residuals of this event are consistent with a location within the transform. The bulletin location may also be mislocated slightly to the east of its true location; the easternmost of the aftershocks would be located east of the mapped intersection [Rusby and Searle, 1995] of the East Pacific Rise and the Anakena transform if the bulletin location were correct. We shifted the location of the reference event shown in Figure 1 twelve km NNW of the bulletin location, placing it and the larger aftershocks within the trough of the Anakena transform.

[8] For the smaller events of the sequence, the only phases that could be detected were T-phases at the quieter OBSs. Consequently, the useful location threshold magnitude is higher than the detection threshold, because distinguishing with confidence between locations on the two transforms requires T-phases or surface waves from stations at a broader range of azimuths than is provided by the OBS array alone.

### 3. Determination of Focal Mechanism and Magnitude

[9] We constrain the focal mechanisms using the radiation patterns of Rayleigh and Love waves as observed on both the OBS array (Figure 2) and at quieter teleseismic stations, which provide broader, but sparser azimuthal coverage. The largest events are all fit well by a double-couple, strike-slip source with one vertical nodal plane that agrees with the strike of the transform and epicentral trend. We measure surface wave magnitude  $M_s$  for the largest event in conventional fashion at multiple, teleseismic stations. For other earthquakes that were large enough to determine the mechanism, the relative magnitude is determined from fitting the radiation pattern at a common set of teleseismic stations.  $M_s$  for events between about 2.8 and 3.3 were determined from Rayleigh waves at RPN only. For events smaller than about 2.8, magnitudes were estimated by extrapolating from the T-phase amplitude using the

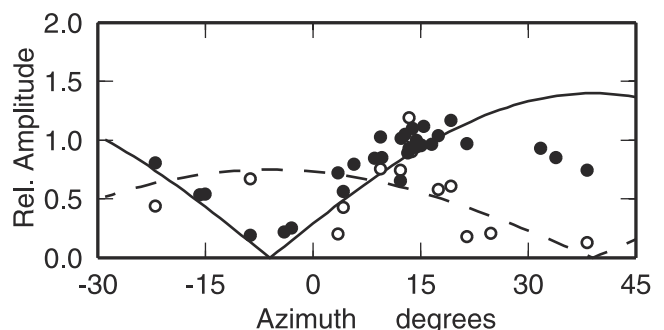


**Figure 2.** Amplitude of surface waves as a function of azimuth from the source. Filled dots are observed Rayleigh amplitudes on the MELT array at frequency 0.04 Hz; open dots are Love at 0.08 Hz; solid line (Rayleigh) and dashed (Love) are prediction for a strike-slip mechanism on a vertical fault striking  $84^\circ\text{E}$  of north. Lateral refraction of waves tends to enhance amplitudes along the strike of the East Pacific Rise, particularly at azimuths of 10 to 15 degrees, and diminish amplitudes at neighboring azimuths [Dunn and Forsyth, 2001].

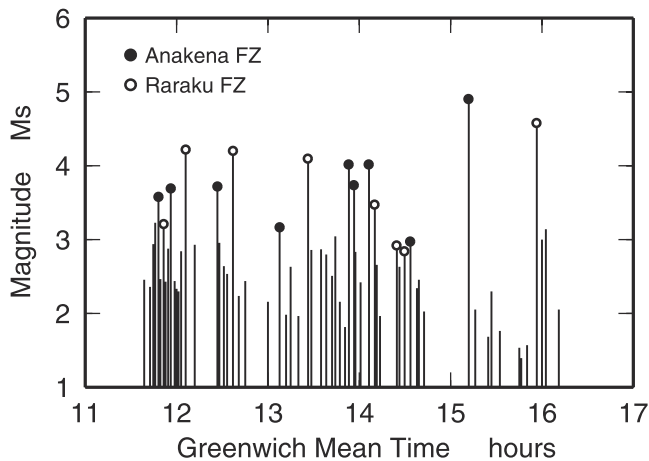


**Figure 3.** Sequence and magnitude of earthquakes in the swarm. Filled or open circles indicate events large enough to be located with enough precision to distinguish between the groupings on the two different transform faults.

$\log(\text{T-phase amplitude})$ -versus- $M_s$  trend found for the larger events.

#### 4. Time Sequence and Location

[10] The epicenters form two clusters striking approximately east-west (Figure 1), in agreement with the strike and separation of the Anakena and Raraku transforms mapped with long-range, side-scan sonar [Searle *et al.*, 1989] and satellite altimetry [Smith and Sandwell, 1997]. These transforms offset the west rift of the Easter microplate and form part of the boundary between the Pacific plate and the microplate. Side-scan sonar shows that both fracture zones have multi-stranded principal-transform displacement zones 5–10 km wide, so the north-south extent of the southern group could represent slip on different strands, rather than errors in location. The seven largest earthquakes of the swarm are all left-lateral, strike-slip events, with the strike of fault planes ranging from about 78 to 85°, approximately parallel to the topographic trends of the transforms. The two aftershocks in succeeding months have similar mechanisms. The slight differences in mechanism are resolvable, but have virtually no effect on the shape of the T-phase envelope or initial phase of Love waves (within a quadrant), so there is no trade-off with location.

[11] The swarm began with a temporally dense cluster of small events (surface wave magnitude  $M_s < 3.7$ ), culminating in a strike-slip event on the Raraku transform ( $M_s 4.2$ ). Most of these initial events could not be located accurately due to their small magnitude and interference with each other's signals, but two of the largest are located near the Anakena transform. Seismic activity continued for the next 2.5 hours at a slightly slower pace, with the larger, locatable events alternating apparently randomly between the two transforms (Figure 3). Then, a 25-minute quiescent period with no shock larger than  $M_s 2.5$  preceded the largest ( $m_b 4.7$ ,  $M_s 4.9$ ) event of the sequence, located on the Anakena transform. The second largest ( $M_s 4.6$ ) earthquake followed 45 minutes later on the Raraku transform, with only a few very small ( $< M_s 3.0$ ) events intervening. Activity continued

for a few more minutes, then ceased on both transforms about 4.5 hours after the beginning of the swarm. The estimated detection threshold using T-phases at the OBS array is about  $M_s 2.5$ . There was one, small, poorly located event about 8.5 hours after the end of the swarm. No other activity was detected until an isolated  $M_s 4.4$  event 67 days later on the Anakena transform. This later event had no detectable foreshocks or aftershocks.

[12] None of the events appear to be located on a spreading center linking the two transforms. The approximate location of the spreading center has been inferred from side-scan sonar [Searle *et al.*, 1989] based on the high acoustic backscattering from young, unconsolidated seafloor, but there has been no detailed mapping in this area. The lack of seismicity does not necessarily indicate the lack of tectonic or volcanic activity on the spreading center. The predicted spreading rate is about 130 mm/yr [Rusby and Searle, 1995], similar to that on the adjacent, fast-spreading East Pacific Rise, which is almost totally aseismic even at the microearthquake level [Shen, 2002]. Given the uncertainty in absolute locations and in location of the spreading center, it is difficult to say whether the southern cluster of earthquakes was east or west of the spreading center or both, but there is an overlap of the two clusters in longitude, suggesting that slip occurred on overlapping, parallel faults rather than being confined to the transform sections of a classic, simple, transform-ridge-transform plate boundary. The north-south separation between clusters is similar to the separation between fracture zone valleys east of 114° 50'W, but resolvably less than the separation to the west of that point.

#### 5. Tectonic Implications

[13] The close temporal coupling of earthquakes on two transforms separated by 20 to 25 km requires a remote, physical coupling of stress and strain on the two faults. Two mechanisms are commonly invoked for triggering of one earthquake by another: changes in the static stress field associated with slip on one fault bringing another pre-stressed fault closer to failure [Reasenber and Simpson, 1992; Stein, 1999]; and dynamic triggering by passage of a transient seismic wave [Hill *et al.*, 1993; Brodsky *et al.*, 2000; Gomberg *et al.*, 2001]. Neither of these mechanisms is likely in this case. Static stress changes are negligible beyond one or two fault lengths from an earthquake; given their small magnitude, the rupture length for any of the events of this study except the largest is unlikely to exceed 1 km. Although the total lengths of the faults affected are greater (minimum along-strike length of 10–15 km for each cluster), the displacement in individual events is so small that the average stress drop would also be very small and static stress changes at a distance of 25 km would be negligible. Coupling begins immediately, before there is any individual earthquake larger than  $M_s 4.0$ .

[14] Dynamic stresses fall off more slowly with distance than static stresses [Scholz, 1998], but the amplitudes of ground motion at a distance of 25 km generated by a magnitude 4 event typical of this swarm would be two to three orders of magnitude smaller than the threshold observed for triggering of remote seismicity by major earthquakes [Hill *et al.*, 1993; Brodsky *et al.*, 2000; Gomberg *et al.*, 2001]. Direct stress triggering by seismic waves can

occur only during the passage of the wave itself and is not observed in this swarm or most other cases of apparent triggering [Scholz, 1998; Gomborg, 2001]. Delayed triggering by dynamic stresses requires some change in the physical properties of the fault or surroundings caused by passage of the seismic wave, such as compaction-induced pore pressure change on a fault [Beeler *et al.*, 2001] or rectified diffusion in a geothermal system [Sturtevant *et al.*, 1996]. The earthquakes in this swarm, except perhaps for the largest event, fall below the magnitude threshold where even self-weakening of faults by dynamic shaking has been observed [Abercrombie, 1995; Brodsky and Kanamori, 2001].

[15] One possible mechanism for generating the apparent seismic coupling of the two transforms is magmatic dike injection along the spreading center linking them. None of the swarm events have been definitely located on a spreading center, but the initial burst of activity may have accompanied intrusion. Although the exact focal mechanisms are not well-constrained, the surface wave radiation patterns of two  $M_s$  3.7 earthquakes within the first hour of the swarm differ from those of the larger events and appear to be consistent with east-west extension on north-south striking normal-faults. There have been many reported examples of volcanic activity being linked to strike-slip earthquakes, particularly in Iceland [e.g., Gudmundsson, 2000]. A dike injected on the Easter-Pacific plate boundary could have been long enough that the static stress field would significantly affect both the Anakena and Raraku faults. On the other hand, dike intrusion on the scale of tens of km normally takes more than a few hours and seismicity triggered by magmatic intrusion may persist for weeks or months, so this suggested mechanism does not explain the short duration of the swarm.

[16] We prefer the explanation that the earthquakes on the Raraku and Anakena transforms are simply the seismic manifestation of a larger, primarily aseismic, slip event involving both transforms. For example, on the San Andreas fault a slow earthquake, or rapid creep event, equivalent to magnitude 4.8, was accompanied by minor local earthquakes up to  $M_L = 3.7$  [Linde *et al.*, 1996]. Although controversial [Abercrombie and Ekstrom, 2001], it has been suggested that some slow earthquakes on the mid-ocean ridge system involve faulting on separate, parallel faults [McGuire *et al.*, 1996; McGuire and Jordan, 2000]. This swarm could be an example of a large, slow event lasting several hours in which only small asperities rupture quickly enough to generate detectable seismic waves. The individual earthquakes do not trigger each other, but are triggered by a common, larger, rapid creep event. If aseismic slip occurred on only one of the faults over a length scale of 10 km or more, the static stress change would favor slip on a parallel fault, but there is no reason why seismicity triggered by static stress changes should be confined only to the duration of active slip on the other fault. The important point for studies of earthquake initiation and prediction is that the coupling or apparent triggering of earthquakes does not have to be self-generated. There may be no direct triggering of one earthquake by another involved in a coupled sequence; a stress or strain episode undetected by ordinary seismological means could trigger all the activity. In this case, the trigger could be a dike

injection event, but more likely it is a largely aseismic, strike-slip, creep episode.

[17] **Acknowledgments.** We thank Christina Rodriguez for help in analysis of the surface wave data. We also thank the OBS groups and the captain and crew of the R/V Melville for their contributions to gathering the data. This work was supported by National Science Foundation grants OCE-9812208 and OCE-9896393 and Defense Threat Reduction Agency contract DTRA01-00-C-0071.

## References

- Abercrombie, R. E., and G. Ekstrom, Earthquake slip on oceanic transform faults, *Nature*, 410, 74–77, 2001.
- Abercrombie, R. E., Earthquake source scaling relationships for  $-1$  to 5 ML using seismograms recorded at 2.5-km depth, *J. Geophys. Res.*, 100, 24015–24036, 1995.
- Beeler, N. M., et al., Compaction-induced pore pressure change: a mechanism to explain dynamic earthquake triggering, *Seismol. Res. Lett.*, 72, 250, 2001.
- Brodsky, E. E., and H. Kanamori, Elastohydrodynamic lubrication of faults, *J. Geophys. Res.*, 106, 16,357–16,374, 2001.
- Brodsky, E. E., V. Karakostas, and H. Kanamori, A new observation of dynamically triggered regional seismicity: Earthquakes in Greece following the August, 1999 Izmit, Turkey earthquake, *Geophys. Res. Lett.*, 27, 2741–2744, 2000.
- Bulletin Int. Seismol. Cent.*, 32, 1995.
- Dunn, R., and D. Forsyth, Short-period Love waves reveal the transition from broad mantle upwelling to the narrow crustal magmatic system beneath the southern East Pacific Rise, *Eos, Eos Trans AGU*, 82, Fall Meet. Suppl., Abs T12A-0898, 2001.
- Gomborg, J., Earthquake triggering by seismic waves following the Landers and Hector Mine earthquakes, *Nature*, 411, 462–466, 2001.
- Gomborg, J., et al., Failure of earthquake failure models, *J. Geophys. Res.*, 106, 16,253–16,263, 2001.
- Gudmundsson, A., Dynamics of volcanic systems in Iceland: Example of tectonism and volcanism at juxtaposed hot spot and mid-ocean ridge systems, *Annu. Rev. Earth Planet. Sci.*, 28, 107–140, 2000.
- Hill, D. P., et al., Seismicity remotely triggered by the magnitude 7.3 Landers, California, earthquake of June 28, 1992, *Science*, 260, 1617–1623, 1993.
- Linde, A. T., et al., A slow earthquake sequence on the San Andreas Fault, *Nature*, 383, 65–68, 1996.
- McGuire, J. J., and T. H. Jordan, Further evidence for the compound nature of slow earthquakes: The Prince Edward Island earthquake of April 28, 1997, *J. Geophys. Res.*, 105, 7819–7827, 2000.
- McGuire, J. J., P. F. Ihmle, and T. H. Jordan, Time-domain observations of a slow precursor to the 1994 Romanche transform earthquake, *Science*, 274, 82–85, 1996.
- MELT Seismic Team, Imaging the deep seismic structure beneath a mid-ocean ridge: The MELT Experiment, *Science*, 280, 1215–1218, 1998.
- Nishimura, C. E., and D. W. Forsyth, The anisotropic structure of the upper mantle in the Pacific, *Geophys. J.*, 96, 203–229, 1989.
- Reasenber, P. A., and R. W. Simpson, Response of regional seismicity to the static stress change produced by the Loma Prieta earthquake, *Science*, 255, 1687–1690, 1992.
- Rusby, R. I., and R. C. Searle, A history of the Easter microplate, 5.25 Ma to present, *J. Geophys. Res.*, 100, 12,617–12,640, 1995.
- Scholz, C. H., Earthquakes and friction laws, *Nature*, 391, 37–42, 1998.
- Searle, R. C., et al., Comprehensive sonar imaging of the Easter microplate, *Nature*, 341, 701–705, 1989.
- Shen, Y., Seismicity at the Southern East Pacific Rise from recordings of an ocean-bottom seismometer array, *J. Geophys. Res.*, in press, 2002.
- Smith, W. H. F., and D. T. Sandwell, Global sea floor topography from satellite altimetry and ship depth soundings, *Science*, 277, 1956–1962, 1997.
- Stein, R. S., The role of stress transfer in earthquake occurrence, *Nature*, 402, 605–609, 1999.
- Stein, R. S., A. A. Barka, and J. H. Dieterich, Progressive failure on the North Anatolian fault since 3939 by earthquake stress triggering, *Geophys. J. Int.*, 128, 594–604, 1997.
- Sturtevant, B., H. Kanamori, and E. E. Brodsky, Seismic triggering by rectified diffusion in geothermal systems, *J. Geophys. Res.*, 101, 25,269–25,283, 1996.

D. W. Forsyth, Y. Yang, and M.-D. Mangriotis, Dept. of Geological Sciences, Brown Univ., Providence, Rhode Island, USA.

Y. Shen, Graduate School of Oceanography, Univ. of Rhode Island, Narragansett, Rhode Island, USA.